Planetary Science and Exoplanets in the Era of JWST
Proceedings IAU Symposium No. 393, 2026
Z. Benkhaldoun, Y. Moulane & A. Szentgyorgyi, eds.
doi:10.1017/S1743921324002722

Advancing Apodization Techniques: Optimizing Interferometric Apodization by Homothety for Exoplanet Detection

A. Qazbour[1,3], Y. El Azhari[1,2,3], J. Chafi[1,3], Z. Benkhaldoun[4], O. Azagrouze[1,2,3] and A. Boskri[1,3]

[1]High Energy Physics and Astrophysics Laboratory, FSSM Cadi Ayyad University, Marrakech, Morocco
email: azizqazbourr@gmail.com

[2]CRMEF-Marrakech Av. Mouzdalifa, BP 797 Marrakech, Morocco

[3]Oukaimeden Observatory, Cadi Ayyad University, Marrakech, Morocco

[4]Sharjah University, United Arab Emirates and University Cadi Ayyad, Morocco

Abstract. New apodization techniques are emerging rapidly to enhance the coronagraphs' rejection capabilities and refine the optics for directly detecting exoplanets. One such technique, Interferometric Apodization by Homothety (IAH), involves splitting the incident Point Spread Function (PSF) into two using a 50 : 50 beamsplitter. One of the resulting PSFs has its amplitude reduced by a factor γ and its transverse dimension expanded by a factor η. By combining these two PSFs, an apodized PSF is generated. In this study, we will use the standard values of γ and η for both rectangular and circular apertures. We implement this approach in the laboratory using a Mach-Zehnder Interferometer with Cube Beamsplitters, chosen for their advantages over Plate Beamsplitters, including easy integration at a 0° angle of incidence and equal optical path lengths for reflected and transmitted light. This technique shows significant promise, achieving a contrast of approximately 5.10^{-3} at small angular separations around 2.8 λ/D.

Keywords. High angular resolution, Apodization, Interferometric Apodization by Homothety "IAH", Exoplanets, Interferometry, Mach-Zehnder interferometer

1. Introduction

Direct detection of exoplanets, especially Earth-like ones, remains a major challenge in modern astronomy due to the high brightness contrast between a star and its orbiting planets (Guyon et al. 2005). The light from a star can be 10^6 more intense than that reflected by its exoplanet in the infrared spectrum and 10^{10} in the visible (Ridgway 2004), which complicate direct imaging. Even advanced instruments struggle to isolate exoplanet light from that of its host star (Traub et al. 2010).

Coronagraphy is a promising solution, it consist to blocks starlight to reveal faint objects like nearby exoplanets. However, managing diffracted light remains a challenge, highlighting the need for apodization (Aime et al. 2001).

Apodization modulates light intensity at the edges of an optical aperture, reducing diffraction and enhancing contrast necessary for exoplanet detection. Integrating an apodizer into a coronagraph significantly improves its abilities to suppress starlight and detect faint planets (Aime et al. 2002).

Improving apodization techniques is central to the scientific community to enhance the telescopes capabilities for future projects. the Habitable Worlds Observatory (HWO)

© The Author(s), 2026. Published by Cambridge University Press on behalf of International Astronomical Union.

https://doi.org/10.1017/S1743921324002722 Published online by Cambridge University Press

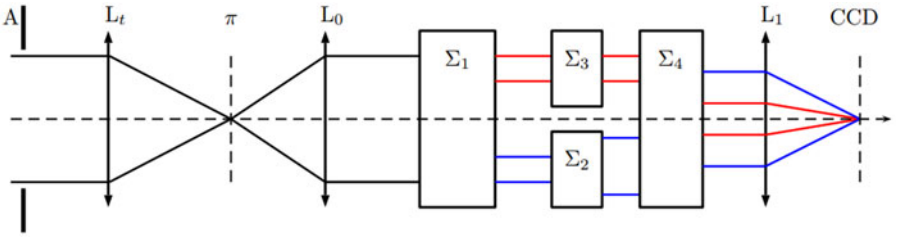


Figure 1. The optical layout of the IAH Principle; A and L_t representing the telescope aperture, π its focal plane. Σ_1 where the amplitude of the incident PSF has splited into two equal PSFs, Σ_2 controle the transverse dimension and the amplitude of one of the two PSFs, Σ_3 componsate for the phase shift introduced by Σ_2, Σ_4 recombine the two PSFs, and finally, the CCD camera where the apodized PSF is formed (Chafi et al. 2023a).

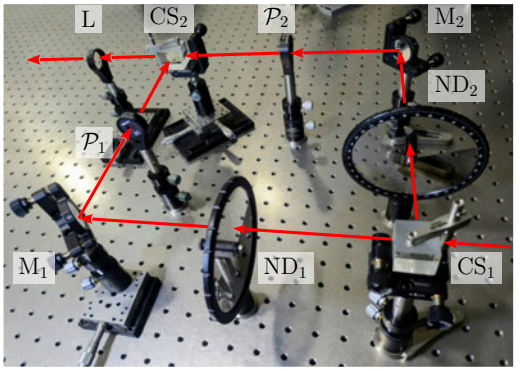


Figure 2. Illustration of the experimental interferometric part of the IAH: the laser light enters into the apodizer from the left (CS_1) and exits from the right (CS_2). The apertures P_1 & P_2 are accurately placed between the first cube beamsplitter CS_1 and the two MZI mirrors M_1 and M_2 respectively, while the two neutral density filters (ND_1 & ND_2) are placed between the last cube beamsplitter (CS_2) and the two MZI mirrors M_1 and M_2 respectively.

project, as recommended in the Astro2020 report (National Academies of Sciences, Engineering, and Medicine 2023). This project aims to directly detect and characterize habitable exoplanets in their star's circumstellar zone (Stark et al. 2024). By combining next-generation coronagraphs with advanced apodization techniques, HWO seeks to overcome technological barriers and usher in a new era of Earth-like exoplanet detection (Belikov et al. 2023).

In our study, we reproduced experimental results reported in Chafi et al. (2023b), using cube beam splitters instead of plate beam splitters, which offer advantages such as easy integration at a 0° angle of incidence, making them a more suitable alternative for direct exoplanet detection experiments.

2. Principle of the technique

IAH consist of splitting the incident PSF into two equal PSFs using amplitude division, The amplitude of one of the resulting PSFs has reduced by a factor γ and its transverse dimension expanded by a factor η, to match its negative lobes with the positive lobes of the second PSF and . By combining these two PSFs, an apodized PSF is generated.

3. Experimental setup

In order to generate the interferometric apodization we use a Mach-Zehnder interferometer with cube beamsplitters instead of plate beamsplitters used by Chafi et al.

https://doi.org/10.1017/S1743921324002722 Published online by Cambridge University Press

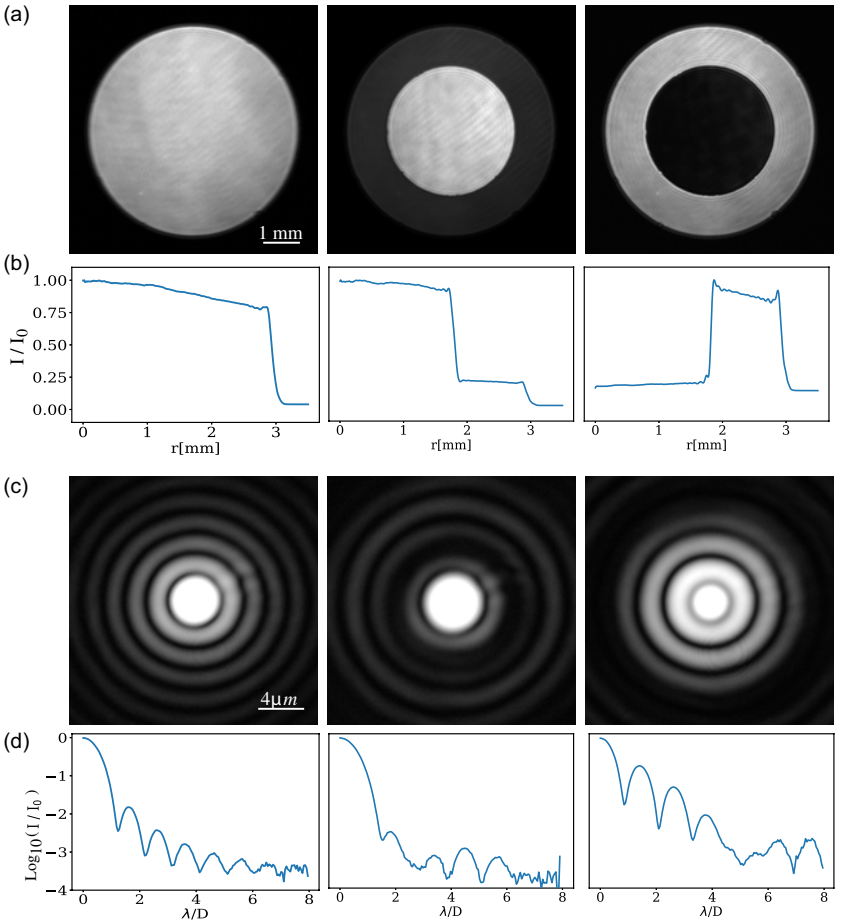


Figure 3. Experimental results for circular aperture; images in the pupil plane (a) and them radial profile (b) PSFs in the focal plane (c) and them radial profile (d). Unapodized (First column), apodized (Second column), and antiapodized (Third column)

(2023b) due to them advantages. The incident beam is splitted into two equal beams, the transverse dimension of one of the PSFs is stretched by the factor η and its amplitude is reduced by the factor γ. The superposition of those two PSFs at the finale focal plane gives an apodized PSF. The Homothety parameters that optimaze the apodization are calculated by Chafi et al. (2023a) for both rectangular and circular apertures.

Figure 2 shows the experimental setup used in this study. As a beam, we use a monochromatic He-Ne laser with a wavelength of 543.5 nm, and a high-resolution camera (SBIG) equipped with a 3326×2504 pixel array KAF-8300 CCD sensor with a surface area of approximately $17.96 \times 13.52\ mm^2$ and 65,000 levels of grayscale.

3.1. *Cube Beamsplitters Advantages*

For this work we choose to use cube beam splitters 'CBS' instead of plate beam splitters 'PBS' due to them advantages. They have an easy integration at a 0° angle of incidence, which permit to avoid the prismatic effect caused by multi reflection inside the PBS. In addition no beam shift, equal optical path lengths, and a shortened optical path.

https://doi.org/10.1017/S1743921324002722 Published online by Cambridge University Press

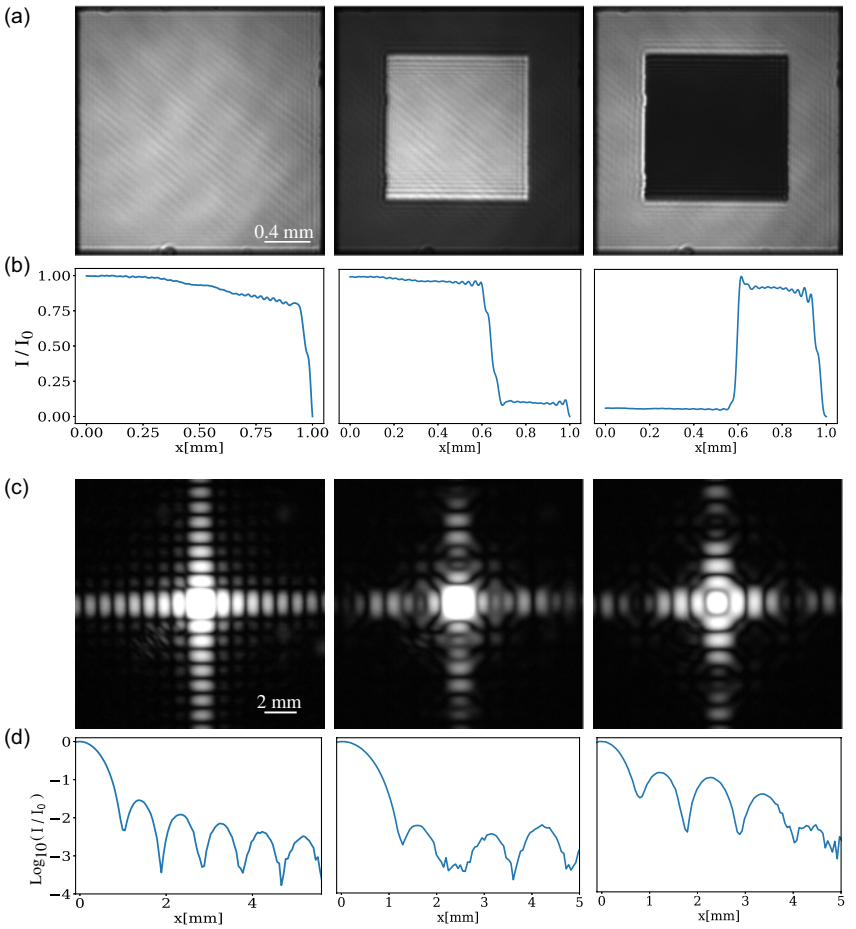


Figure 4. Experimental results for rectangular aperture; images in the pupil plane (a) and them transverse cross-sections along the horizontal axis (b) PSFs in the focal plane (c) and them transverse cross-sections along the horizontal axis (d). Unapodized (First column), apodized (Second column), and antiapodized (Third column)

4. Experimental results

At first, we place the CCD camera at the pupil plane, then we move it to the focal plane to capture the PSFs.

For this experimental study, we use the standard values calculated by Chafi et al. (2023a) for the parameters γ and η for both rectangular and circular apertures. All the images are taken with 0.9s exposure time.

4.1. *Circular aperture*

The objectif of this paragraph is to see the final results in the focal and the pupil planes, to compare them with Chafi et al. (2023b) results.

The CCD camera is initially placed at the pupil plane. Line (a) shows the pupil images, and line (b) presents their corresponding radial profiles. The CCD camera is then moved to the focal plane; line (c) shows the PSFs (Point Spread Functions), and line (d) presents their radial profiles. The first column corresponds to the unapodized pupil, the second column to the apodized pupil (destructive interferometry), and the third column to the anti-apodized pupil (constructive interferometry) (see figure 3).

https://doi.org/10.1017/S1743921324002722 Published online by Cambridge University Press

As shown in the figure, this technique can attend a contrast of approximately 5.10^{-3} at small angular separations around 2.8 λ/D.

4.2. *Rectangular aperture*

We will do the same as in the case of circular aperture; we replace the circular apertures by the rectangular apertures and we change the values of the filters to correspond to those used by Chafi et al. (2023a).

By repeating the same process as in the case of circular aperture the CCD camera is placed in the pupil plane. Line (a) presents the pupil images, line (b) them transverse cross-sections along the horizontal axis, while Line (c) presents the PSFs, and line (d) them transverse cross-sections along the horizontal axis. First column unapodized pupil, second column apodized pupil, and third column antiapodized pupil (see figure 4).

5. Conclusion

Our study demonstrates the effectiveness of interferometric apodization by homothety in enhancing the capabilities of exoplanet detection. By employing a Mach-Zehnder interferometer with cube beamsplitters, we tried to optimize the concentration of light in the central diffraction lobe, and achieve notable efficiency for both circular and rectangular apertures. The experimental results show a contrast of approximately 5.10^{-3} around 2.8 λ/D for circular aperture, which can improve the sensitivity and rejection capabilities of coronagraphs. The use of CBS instead of PBS, this technique proves to be promising for future integration with advanced telescopes. By increasing the contrast and detection capabilities at small angular separations, our method holds significant potential for improving upcoming exoplanet observation missions. In the coming months, we will focus on evaluating the performance of this approach using a white light source.

References

Aime, C., Soummer, R., & Ferrari, A. 2001, AAP, 379, 697. doi:10.1051/0004-6361:20011293

Aime, C., et al. A&A, 2002. doi:10.1051/0004-6361:20020419

Belikov, R., et al. In: Techniques and Instrumentation for Detection of Exoplanets XI, SPIE, vol. 12680, p. 126802G, 2023. doi:10.1117/12.2677732

Chafi, J., et al. MNRAS, vol. 523, no. 4, pp. 5442–5451, 2023

Chafi, J., et al. MNRAS, vol. 527, no. 3, pp. 7036–7046, 2023

Gaudi, B. S., et al. arXiv e-prints, 2020, arXiv:2001.06683

Guerri, G., et al. Experimental Astronomy, vol. 30, no. 1, pp. 59–81, 2011

Guyon, O., et al. (2005). "Exoplanet Imaging with a Phase-induced Amplitude Apodization Coronagraph. I. Principle." The Astrophysical Journal, 622(1), 744–758

Habib, A., et al. MNRAS, vol. 406, no. 4, pp. 2743–2748, 2010. doi:10.1111/j.1365-2966.2010.16873.x

Juanola-Parramon, R., et al. Journal of Astronomical Telescopes, Instruments, and Systems, vol. 8, p. 034001, 2022. doi:10.1117/1.JATIS.8.3.034001

National Academies of Sciences, Engineering, and Medicine. The National Academies Press, Washington, DC, 2023, doi:10.17226/26141

Ridgway, S. T. 2004, EAS Publications Series, 12, 49. doi:10.1051/eas:2004023

Stark, C. C., Mennesson, B., Bryson, S., et al. 2024, arXiv:2405.19418. doi:10.48550/arXiv.2405.19418

Traub, W. A., Oppenheimer, B. R. (2010). "Direct Imaging of Exoplanets." In Exoplanets, ed. S. Seager (Tucson: University of Arizona Press), 111–156

https://doi.org/10.1017/S1743921324002722 Published online by Cambridge University Press